C. R. Chimie 20 (2017) 818–826

Contents lists available at ScienceDirect

Comptes Rendus Chimie

www.sciencedirect.com

Full paper/Mémoire

Efficient cenosphere supported catalyst for the esterification of *n*-octanol with acetic acid

Vishal S. Chandane, Ajit P. Rathod*, Kailas L. Wasewar, Shriram S. Sonawane

Department of Chemical Engineering, Visvesvaraya National Institute of Technology, Nagpur 440010, MS, India

ARTICLE INFO

Article history:
Received 17 January 2017
Accepted 16 March 2017
Available online 18 April 2017

Keywords:
Cenosphere
Heterogeneous catalyst
Response surface methodology
Esterification
n-Octyl acetate

ABSTRACT

An efficient heterogeneous acid catalyst was developed using cenospheres, a byproduct of coal-fired thermal power plants by the method of wet impregnation. Catalyst characterization was carried out using various analytical techniques, namely, Fourier transform infrared, X-ray diffraction, field emission gun scanning electron microscopy and Brunauer–Emmett–Teller surface area and surface acidity analysis. The characterization revealed the excellent catalytic activity of the catalyst for the esterification reaction of *n*-octanol and acetic acid. Various reaction parameters, namely, catalyst loading, a molar ratio of alcohol/acid and reaction temperature were evaluated and optimized by response surface methodology using the Box–Behnken model. The response surface methodology model equations corresponding to the conversion of acid and % yield of ester were developed. The model well predicted the optimal reaction conditions, which were validated experimentally with good agreement. The excellent catalytic performance was observed in the esterification reaction with high conversion of acid (95.34%) and high yield of *n*-octyl acetate (94.81%). Reusability study of the catalyst showed that the catalyst could be used efficiently up to three reaction cycles. This study explores the use of cenospheres to prepare a solid acid catalyst for the industrially important esterification reactions.

1. Introduction

Cenosphere is a coal combustion byproduct, generated abundantly in coal burning thermal power plants. It consists essentially of silica and alumina along with some traces of oxides of Ca, Mg, Na, Mn, Fe and Ti [1]. The constant generation of cenospheres in huge amounts posed a challenge to waste disposal and environmental management. One feasible way to treat this huge amount of cenospheres is by its recycle. Among the large amounts of cenospheres, a small portion is used as building materials and production of ceramic materials [2]; however, there is still a portion that is being disposed of in the landfills and ponds [3]. Thus, the development of the environmentally safe application of cenosphere is very essential. Research efforts are directed towards the alternative methods for disposal of cenosphere, its proper usage by exploring new applications and identifying new ways of recycling. In view of that, the disposal and recycle of cenospheres have attracted a great deal of interest owing to its low density, stability, nontoxic nature and strong filling ability [4]. Cenosphere is used as substrate in the studies such as zeolites [5], core–shell structure [6], geopolymeric composites [7] and catalyst support [8,9]. However, the search for newer applications of cenosphere is still ongoing.

The products of esterification reactions are widely applied as flavors, fragrances and perfumeries in several chemical industries [10]. Homogeneous acid catalysts such as sulfuric acid, phosphoric acid and *p*-toluene sulfonic acid are used to obtain esterification products. The main

* Corresponding author.
E-mail addresses: ajitprathod@gmail.com, ajitprathod@rediffmail.com (A.P. Rathod).

http://dx.doi.org/10.1016/j.crci.2017.03.007
1631-0748/

drawbacks of this production process are high corrosiveness to the equipment, non-reusability of acid catalysts, extra purification steps and environmental troubles [11,12]; as a result, a huge quantity of environmental acidic waste is produced [2]. Heterogeneous solid catalysts are developed for the sustainable production of esters. These solid heterogeneous catalysts provide significant stability and activity, easy separation from the reaction mixture, reusability and do not cause any corrosion problem to the equipment [13]. In this context, solid acid catalysts such as zeolites, sulfated zirconia and acidified silica have been used. The esterification reactions catalyzed by $SO_4^{2-}/Al_2O_3–SiO_2$ catalyst [14], zinc oxide [15], cobalt oxide [16] and sulfated zirconia [17,18] are reported in recent years. In addition, supported ionic liquids [19,20], supported montmorillonite K10 [21,22], supported palladium [23], sulfated Si-doped zirconia [24] and sulfonated carbon [25,26] have been used as an efficient and active heterogeneous catalyst for the various esterification reactions.

Cenospheres are referred as fly ash cenospheres (FACs), mainly composed of the high amount of silica and alumina with few traces of Fe_2O_3 and TiO_2. It can be used as a catalyst or catalytic support for the esterification reaction because of its high silica content, which is associated with a significant amount of surface acidity. FAC is a very low-cost and abundantly available waste material. Most of the elements including alumina and Fe present in FACs are leached out during the acid treatment. As a result, the silica content of FACs is increased, which subsequently enhances the surface acidity [27]. Moreover, FACs possess unique properties like light weight, constant spherical structure and good mechanical, chemical and thermal stability. In addition, the high silica content facilitates in catalysis of various chemical reactions and also provides support to different catalytic species on the surface [28]. Owing to these highly significant characteristics, FACs are believed to be a significant material for the synthesis of a heterogeneous catalyst. Earlier, the authors reported an efficient solid acid catalyst by using fly ash as a catalytic support for transesterification reactions [3,29]. However, to the author's knowledge, no information is available in the open literature describing the application of the FAC-supported heterogeneous catalyst for the esterification reaction to synthesize flavor esters. In view of above, an attempt is made to develop a suitable, efficient and cost effective FAC-based catalyst for the esterification reaction. The ester synthesized in the present esterification reaction is *n*-octyl acetate, which has an odor reminiscent of oranges and grapefruits. This ester is widely applied as an artificial flavor and also as a solvent in many chemical industries.

In the present work, for the first time the FAC-supported heterogeneous acid catalyst was prepared by impregnating it with ammonium sulfate. The catalyst was synthesized by a low-cost method using a cost-effective precursor, and it is used in the synthesis of high-value product viz., ester. The prepared catalyst was characterized and its catalytic performance was investigated in the esterification of *n*-octanol and acetic acid. With the aim of optimizing the conversion of acetic acid and % yield of ester, the effects on various process parameters, namely, catalyst loading, molar ratio of alcohol/acid and reaction temperature were investigated, and the optimal reaction conditions corresponding to maximum conversion of acetic acid and % yield of ester were determined using response surface methodology with the Box–Behnken Design (BBD).

2. Experimental section

2.1. Chemicals and materials

FACs were collected from Vipra Ferro Alloy Pvt. Ltd. (Nagpur, Maharashtra, India), which contains approximately 70% ($SiO_2 + Al_2O_3 + Fe_2O_3$). Before its use, it was sieved to a size of <100 μm. Acetic acid (purity >99%) was purchased from Merck, and *n*-octanol (purity >99%) was obtained from Loba Chemie Pvt. Ltd. (Mumbai, India). Ammonium sulfate (purity >99.5%) was procured from Fisher scientific, India. Methanol (purity >99%) and Karl Fischer reagent were procured from Rankem Chem. Ltd. (Mumbai, India). *n*-Hexane (GC grade, purity >99%) was procured from Sigma–Aldrich. All of the chemicals used in this study were of analytical reagent grade. Deionized, double distilled water was used in the experiments.

2.2. Synthesis of solid acid catalyst

The FAC-supported solid acid catalyst was synthesized by the method of wet impregnation. The required amounts of the aqueous stock solution of ammonium sulfate were laden onto different quantities of FACs with a constant manual stirring. Particularly, 15.4 mL of an aqueous stock solution of ammonium sulfate was added gradually to 15 g of FACs with constant stirring. The mixture was stirred properly to fill up the pores of FACs. Then, it was kept for drying in hot air oven at 80 °C for about 2 h. The dried material was then calcined in a muffle furnace at 400 °C for 4 h. Finally, the calcined material was stored in a dry storage bottle before using it for the esterification reaction.

2.3. Catalyst characterization

Powder X-ray diffraction (XRD; PANalytical 3 kW X'pert Powder) was performed for the identification of crystalline nature and crystalline size of the FAC-supported solid acid catalyst. XRD was performed using Cu Kα radiation ($\lambda = 1.5406$ Å) with a generator setting of 30 mA and 40 kV. The XRD patterns were recorded in the 2θ range of 10–100° with a scanning speed of $0.1°s^{-1}$. The crystalline size was determined by the Debye–Scherrer equation:

$$B = 0.9\lambda/\beta \cos\theta \quad (1)$$

where B represents the crystalline size, λ is the X-ray wavelength (1.54 Å for Cu Kα), β is the broadening of the peak (measured as full width at half-maximum intensity) and θ represents the peak position.

Fourier transform infrared (FTIR equipped with attenuated total reflection) (Thermo Scientific iD5) spectroscopic measurements were carried out for the identification of surface functional groups of the FAC-supported solid acid catalyst. The FTIR spectra were recorded in the range of 400–4000 cm^{-1}.

The specific surface area of the FAC-supported solid acid catalyst was determined by the single point BET (Brunauer–Emmett–Teller) method (Smart Instruments Co. Pvt. Ltd., Mumbai, India) using a nitrogen adsorption–desorption technique.

The surface morphology of the FAC-supported solid acid catalyst was examined by the field emission gun scanning electron microscopy (FESEM) at 15 kV (Hitachi, S-4800, Japan). Samples were coated with a thin gold film before observing the micrograph.

The total surface acidity was quantified by the titration method. One gram of the catalyst was dispersed in a 50 mL of 1 M sodium chloride solution. It was then subjected to sonication for 1 h. After this, the catalyst was filtered and separated. The filtrate solution was titrated against 0.1 N sodium hydroxide solution using a phenolphthalein indicator.

2.4. Catalytic performance of solid acid catalyst in esterification

The performance of the solid acid catalyst was evaluated in esterification of acetic acid with *n*-octanol to yield *n*-octyl acetate and water (Scheme 1). The esterification was performed in a reactor consisting of a three-neck Borosil glass flask (250 mL) fitted with a reflux condenser. The flask was heated on a rotamantle, and the temperature inside the reactor was controlled by proportional–integral–derivative temperature controller (accuracy ± 1 °C). The content inside the flask was stirred with a magnetic stirrer. In a typical run, *n*-octanol was first charged into the reactor and heated to the desired temperature under reflux. After the desired temperature was reached, preheated acetic acid was added to the reactor followed by the addition of the solid acid catalyst. About 1 mL of a liquid sample was taken out from the reactor at regular time intervals.

2.5. Analysis

The samples taken periodically were analyzed by the method of titration, Karl Fischer titration and gas chromatography (GC). The residual acid content was evaluated by titration, which was carried out with 0.1 N sodium hydroxide solution using phenolphthalein as an indicator. The sodium hydroxide solution was standardized by 0.1 N oxalic acid.

Water formed during the reaction was analyzed by Microprocessor-based Karl Fischer titrator (Optics Technology, India). GC (Thermo Scientific Trace 1110) equipped with a flame ionization detector and provided with a capillary column BP 20 (SGE Analytical Science, 25 m × 0.22 mm × 0.25 μm) was used to determine the composition of the reaction mixture. The samples were diluted in *n*-hexane before injecting to GC and high purity N_2 was used as a carrier gas at a flow rate of 2 mL/min. In each analysis, 2 μL of a sample was injected and the split ratio was adjusted to 10:1. The results of titration, Karl Fischer method and GC were compared and found to be within ± 1.5%.

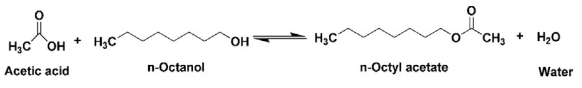

Scheme 1. General reaction mechanism of Acetic acid and *n*-Octanol.

2.6. Experimental design and statistical analysis

The experimental design for the solid acid catalyst to study its performance in the esterification reaction was performed through the BBD using Design-Expert software (V10, State-Ease Inc., USA). The design involved three process parameters (independent variable) viz., catalyst loading, alcohol/acid molar ratio and reaction temperature and two response variables viz., % conversion of acid and % yield of ester. Each factor with their coded and uncoded values is presented in Table 1.

A total of 17 sets of individual experiments (12 factorial points and five centre points) were performed according to the standard BBD. The experiments were performed in a randomized order as generated by Design-Expert software to avoid the bias. In each case, % conversion of acid and % yield of ester were determined. The complete experimental design together with results is presented in Table 2. The experimental data were analyzed by a second-order polynomial equation relating process variables and response variables, which is as follows:

$$Y = \beta_0 + \sum_{i=1}^{3} \beta_i X_i + \sum_{i=1}^{k} \beta_{ii} X_i^2 + \sum_{i=1}^{2} \sum_{j=i+1}^{3} \beta_{ij} X_i X_j \quad (2)$$

where Y is the response variable, β_0, β_i, β_{ii} and β_{ij} are the intercept, linear, quadratic and interaction effect coefficients, respectively. The statistical analysis of the work was performed through analysis of variance (ANOVA) and accuracy of the model was evaluated by the coefficient of determination, R^2. The statistical significance of the model and the coefficients of model equation were tested by the F value.

3. Results and discussion

3.1. Characterization of solid acid catalyst

3.1.1. Physicochemical characterization

FTIR spectroscopic analyses of pristine FACs and the FAC-supported solid acid catalyst are shown in Fig. 1a and b.

The pristine FACs (Fig. 1a) show the presence of bands at 1032 and 798 cm^{-1}, which can be assigned to asymmetric and symmetric Si–O–Si stretching modes, respectively. The FTIR band at 554 cm^{-1} is attributed to asymmetric stretching vibrations of Si–O–Al present in the aluminosilicate structure. In addition, the band at 3442 cm^{-1} is because of the hydroxyl group of silanols (–Si–OH).

Table 1
Process variables and their levels used in BBD.

Variables	Symbol	Coded levels		
		−1	0	+1
Catalyst loading (wt %)	X_1	1	3	5
Molar ratio of alcohol/acid	X_2	1	1.5	2
Reaction temperature (°C)	X_3	70	90	110

Table 2
BBD, experimental and predicted values of conversion of acid and % yield of ester for three process variables.

Run	Experimental variables			Conversion (%)		% Yield	
	X_1	X_2	X_3	Experimental	Predicted	Experimental	Predicted
1	3	1.5	90	71.78	71.78	70.25	70.26
2	3	1.5	90	71.78	71.78	70.25	70.26
3	5	1.5	70	75.4	75.92	74.86	75.28
4	3	2	70	77.18	76.28	75.95	75.16
5	5	1	90	66.25	66.01	65.66	65.18
6	3	1.5	90	71.78	71.78	70.25	70.26
7	3	1.5	90	71.78	71.78	70.25	70.26
8	3	1	110	75.13	76.03	74.37	75.17
9	3	1.5	90	71.78	71.78	70.25	70.26
10	3	2	110	95.34	95.62	94.81	94.74
11	3	1	70	56.7	56.42	55.17	55.25
12	1	2	90	78.11	78.35	76.87	77.36
13	5	2	90	85.32	85.71	84.00	84.38
14	1	1.5	110	88.53	88.01	87.88	87.47
15	5	1.5	110	93.26	92.60	92.57	92.26
16	1	1.5	70	65.08	65.74	64.62	64.94
17	1	1	90	58.99	58.61	57.45	57.07

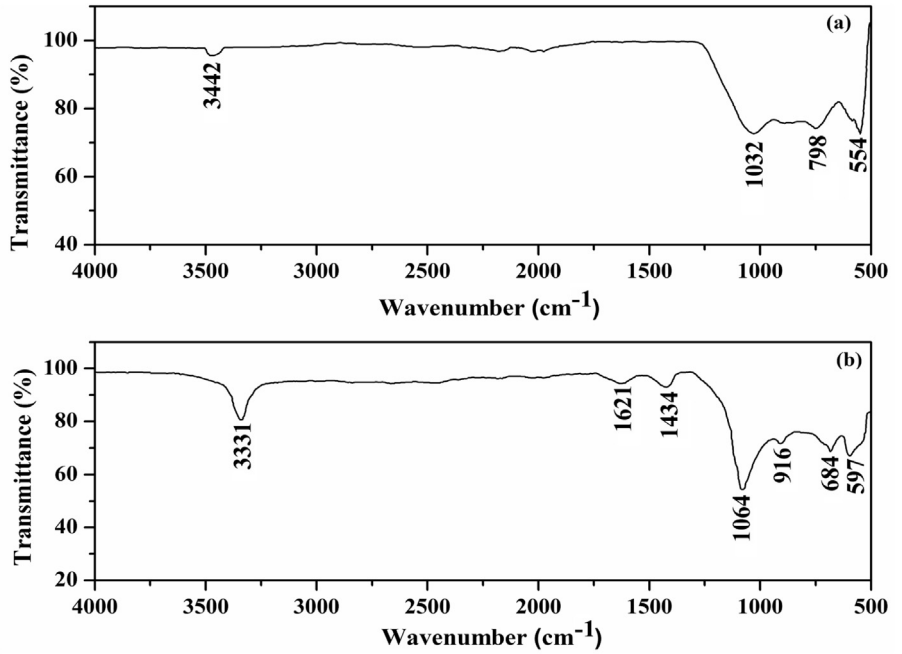

Fig. 1. FTIR spectrum of (**a**) pristine FACs and (**b**) FAC-supported solid acid catalyst.

Similarly, the bands at 1064, 684 and 597 cm^{-1} in the FTIR spectrum of the FAC-supported solid acid catalyst (Fig. 1b) are assigned to asymmetric Si–O–Si, asymmetric Si–O–Si and asymmetric Si–O–Al stretching modes, respectively. In addition, the bands are observed at 916 and 1434 cm^{-1}, which can be attributed to symmetric vibrations of S–O and Si–O–S, respectively. This revealed impregnation of sulfate ions on the surface of the FAC-supported solid acid catalyst. The bands at 3331 and 1621 cm^{-1} are because of the –OH stretching and bending vibrations, respectively. It is observed that the peak intensity of –OH band at 3331 cm^{-1} is stronger in the FAC-supported solid acid catalyst (Fig. 1b) than that of in pristine FACs (Fig. 1a), which indicated that more –OH groups are introduced in the FAC-supported solid acid catalyst [2]. This broad and intense band for the –OH group is because of the increase in silica content upon treatment of impregnation [3,30].

The BET surface area obtained from the nitrogen adsorption–desorption method was found to be 1.19 m^2/g for the FAC-supported solid acid catalyst and 0.35 m^2/g for pristine FACs. The surface area of the FAC-supported solid acid catalyst was enhanced, which revealed the availability of more acidic sites for the esterification reaction [2].

The total surface acidity of the FAC-supported solid acid catalyst quantified by the titration method was calculated as 2.81 ± 0.59 mmol/g. This reveals that FAC-supported catalyst possessed sufficient acidity to catalyze the esterification reaction.

3.1.2. Mineralogical characterization

The XRD pattern of pristine FACs and FAC-supported solid acid catalyst is represented in Fig. 2a and b. Fig. 2a and b shows the presence of orthorhombic mullite (JCPDS Card No. 79-1457) and hexagonal quartz (JCPDS Card No. 83-2465) both in pristine FACs and the FAC-supported solid acid catalyst. This reveals that FAC particles are mainly composed of a mixture of mullite and quartz. However, a substantial amount of sulfate species (JCPDS Card No. 33-1285) is observed in the solid acid catalyst. A decline in intensity of diffraction peaks of mullite and quartz, and an introduction of diffraction peaks of new sulfate species in the XRD pattern of the FAC-supported solid acid catalyst indicated that some of the crystalline components of pristine FACs were eliminated during the impregnation process. Because of this, the percentage of silica content increased and crystallinity gets reduced in the solid acid catalyst as compared with that of pristine FACs [31]. The crystalline size estimated from the Debye–Scherrer equation is evaluated as 8 nm showing the presence of nanocrystalline phase in the solid acid catalyst.

3.1.3. Morphological characterization

FESEM images of pristine FACs and the FAC-supported solid acid catalyst are presented in Fig. 3a and b. The FESEM micrograph of pristine FACs (Fig. 3a) shows the presence of spherical particles with a smooth morphology. However, after impregnation, the FESEM micrograph (Fig. 3b) of the FAC-supported solid acid catalyst shows the agglomeration of fine particles on the surface in a random manner. This revealed that process of impregnation imparted new acidic sites on the surface of FACs. This result is well supported by FTIR and XRD analysis. It was also observed that the impregnation on FACs did not show any disruption in the structural morphology of FACs used as a support, whereas the agglomerated surface morphology of the FAC-supported solid acid catalyst may be responsible for the enhancement of BET surface area.

3.2. Effect of ammonium sulfate loading

The effect of loading of ammonium sulfate on the FAC-supported solid acid catalyst was observed and optimized in the esterification of acetic acid and *n*-octanol. For this purpose, the esterification reaction was carried out at an alcohol/acid molar ratio of 2, catalyst amount of 5 (wt %) and the reaction temperature of 110 °C.

Fig. 4 elucidates the conversion of acetic acid by varying ammonium sulfate loading on the FACs. As can be seen, with the increase in ammonium sulfate loading from 10 to 25 wt %, the conversion of acetic acid increased from 72.35% to 94.27%. After loading of 25 wt %, a minute increase was observed. Thus, 25 wt % of ammonium sulfate loading was used for optimizing other process parameters.

3.3. Model fitting and ANOVA

The experimental data obtained according to the standard BBD are tabulated in Table 2. A considerable variation was observed in the conversion of acid and % yield of ester

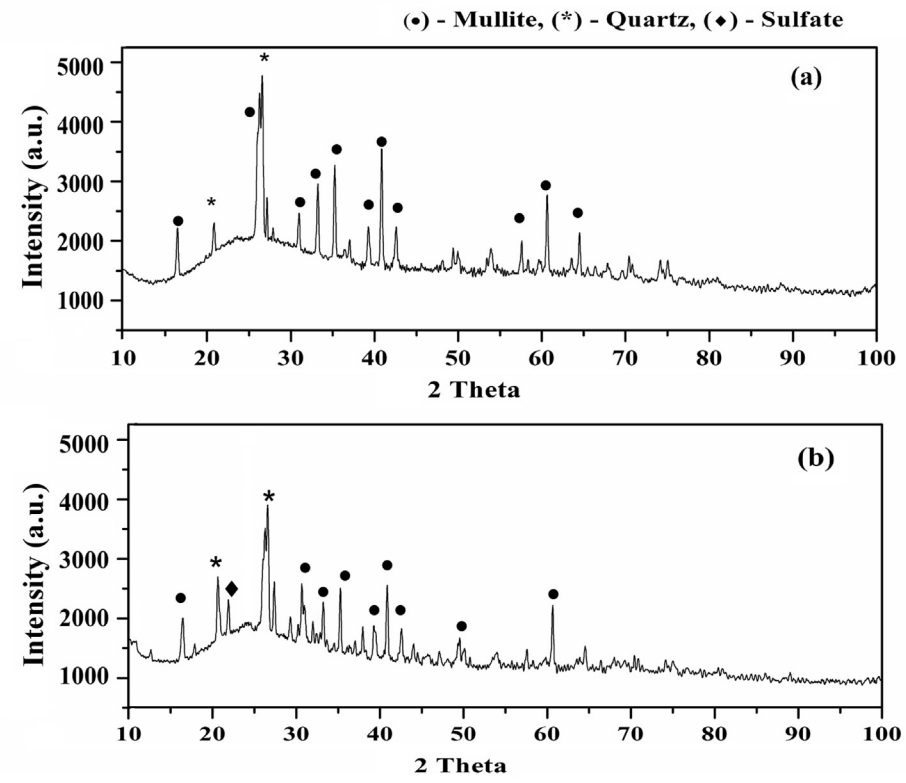

Fig. 2. XRD pattern of (**a**) pristine FACs and (**b**) FAC-supported solid acid catalyst.

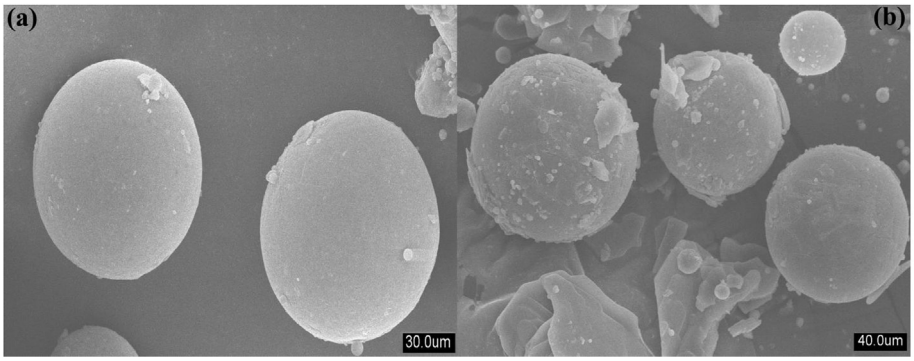

Fig. 3. FESEM images of (**a**) pristine FACs and (**b**) FAC-supported solid acid catalyst.

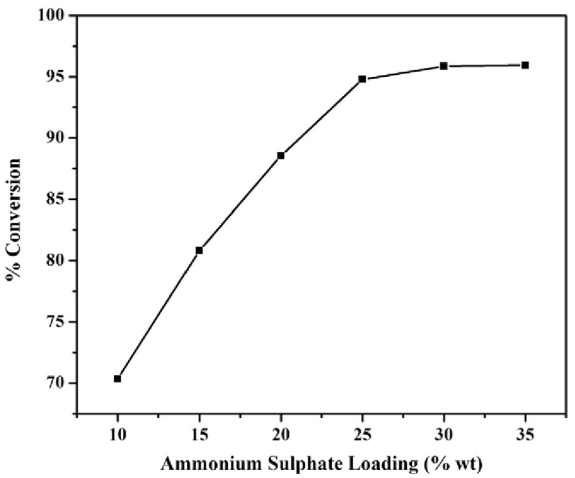

Fig. 4. Variation of ammonium sulfate loading on FACs and its effect on the % conversion of acid.

under different process conditions. The conversion of acetic acid obtained was ranged from 58.99% to 95.34% and % yield was ranged from 57.45% to 94.81%. Two second-order polynomial equations for two response variables predicted by software depicting the relationship between process parameters and response variables in terms of actual factors are given as

$$Y = 98.1687 + 1.3575X_1 + 44.92X_2 - 2.2573X_3 + 0.6084X_1^2 - 8.185X_2^2 + 0.0158X_3^2 - 0.0125X_1X_2 - 0.034X_1X_3 - 0.006X_2X_3 \quad (3)$$

$$Y = 4513.57 + 105.61X_1 + 23.17\,X_2 - 29.27\,X_3 - 0.294X_1^2 - 1.662X_2^2 + 0.0473X_3^2 - 0.0187X_1X_2 - 0.0203X_1X_3 - 0.2927X_2X_3 \quad (4)$$

The terms with a positive sign in Eqs. 3 and 4 indicate the linear effect and the terms with a negative sign indicate the antagonistic effect [29]. It can be seen that the molar ratio is linearly affecting the esterification followed by catalyst loading. In particular, the molar ratio had the highest effect on the conversion of acetic acid and % yield of the ester. The relationship between experimental and predicted values of the developed model equations is demonstrated in Fig. 5a and b. The figure depicted a good linear correlation indicating that the models were successful in demonstrating the relationship between three process variables and the response variables. The statistical significance of each parameter was evaluated by the ANOVA test. The ANOVA test results are tabulated in Table 3.

The result in Table 3 reveals the statistical significance of each process variables and their interactions at 95% confidence level. As can be seen from Table 3, the *P* value of the model is <0.0001 for both cases, which suggest that the models are highly significant. The *F* value of model corresponding to the conversion of acetic acid is 402.17 and to yield is 581.91. This large *F* value indicated that the model is significant and there is 0.01% chance that the large *F* value could occur because of noise. The R^2 values of 0.9980 and 0.9986 revealed that the model can explain 99.80% and 99.86% of target function variables. The adjusted R^2 values of 0.9955 and 0.9969 demonstrated an excellent correlation between independent variables. The predicted R^2 values of 0.9691 and 0.9786 were in reasonable agreement with respective adjusted R^2 values as their differences are less than 0.3. In addition, the *P* values of X_1, X_2, X_3, X_1X_3, X_1^2, X_2^2 and X_3^2 are less than 0.05, which revealed that these variables were significantly important in affecting the conversion of acid and % yield of ester. Furthermore, the quadratic effect of X_3^2 had the largest effect than other quadratic effects. In addition, the interaction effect of catalyst loading (X_1) and temperature (X_3) had a higher effect than that of other interaction effects.

3.4. Optimal reaction condition and model validation

The optimal reaction conditions for the esterification reaction catalyzed by the solid acid catalyst were determined by the numerical feature of Design-Expert software. In a typical feature, the process variables were set within their minimum and maximum range (Table 1), and the response variables were set for maximization. The optimal reaction conditions were found as follows: catalyst loading,

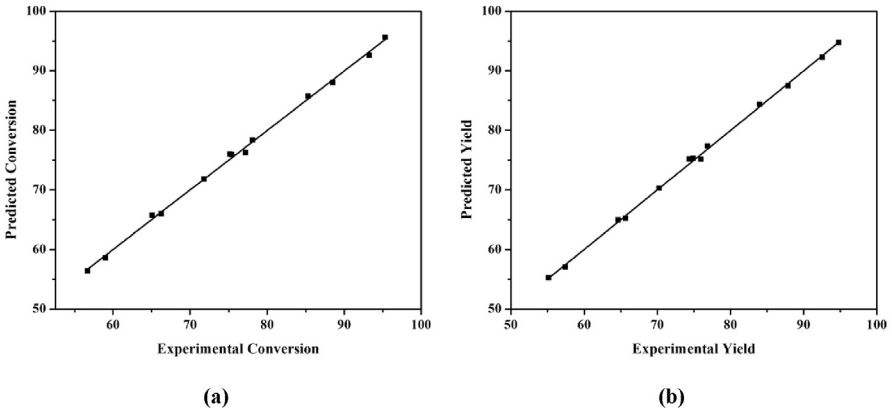

Fig. 5. Predicted vs experimental (**a**) % conversion of acid and (**b**) % yield of ester.

Table 3
ANOVA for acquired model.

Conversion (%)				% Yield			
Source	Std error	*F* value	*P* value	Source	Std error	*F* value	*P* value
Model	0.3210	402.17	<0.0001	Model	0.2719	581.91	<0.0001
X_1	0.2538	211.33	<0.0001	X_1	0.2149	309.70	<0.0001
X_2	0.2538	1508.91	<0.0001	X_2	0.2149	2108.41	<0.0001
X_3	0.25383	1471.65	<0.0001	X_3	0.2149	2110.91	<0.0001
X_1X_2	0.3589	0.0012	0.9732	X_1X_2	0.3040	0.7993	0.4010
X_1X_3	0.3589	15.155	0.0060	X_1X_3	0.3040	20.823	0.0026
X_2X_3	0.3589	0.0353	0.8562	X_2X_3	0.3040	0.0806	0.7847
X_1^2	0.3498	48.384	0.0002	X_1^2	0.2963	90.888	<0.0001
X_2^2	0.3498	34.203	0.0006	X_2^2	0.2963	49.451	0.0002
X_3^2	0.3498	329.773	<0.0001	X_3^2	0.2963	543.11	<0.0001
Residual	3.608			Residual	2.588		
Lack of fit	3.608			Lack of fit	2.588		
Pure error	0			Pure error	0		
Cor total	1869.29			Cor total	1938.98		
$R^2 = 0.9980$, adjusted $R^2 = 0.9955$, predicted $R^2 = 0.9691$				$R^2 = 0.9986$, adjusted $R^2 = 0.9969$, predicted $R^2 = 0.9786$			

4.83 (wt %); alcohol/acid molar ratio, 1.9 and reaction temperature, 108 °C. The predicted values of conversion of acetic acid and % yield of the ester under these conditions were 97.82% and 96.96%, respectively. The optimal conditions predicted by the software were validated experimentally.

Three independent experiments were performed under the optimal process conditions, the % conversion of acetic acid and % yield of ester at the optimal conditions were found to be (96.84 ± 0.85)% and (95.72 ± 1.26)%, respectively. Because the interaction of catalyst loading and the reaction temperature was significant as per ANOVA (Table 3), the contour plots were constructed by keeping the alcohol/acid molar ratio at an optimal level. The contour plots are shown in Fig. 6a and b, which revealed that an increase in catalyst loading increases the % conversion of acetic acid and % yield of ester. With increasing the catalyst loading, the number of active catalytic sites increased, which subsequently gave more amount of product. Similarly, increase in reaction temperature also enhanced the % conversion of acetic acid and % yield of ester. The raising temperature drives the equilibrium towards the formation of products as the esterification reaction is endothermic [29]. The nature of the contour plot is elliptical, which suggested a significant interaction between the parameters as elucidated by ANOVA.

3.5. Catalyst activity

To evaluate the catalytic activity, the performance of the FAC-supported catalyst was compared with other homogeneous and heterogeneous catalysts, namely, H_2SO_4 and Amberlyst 15. Under the optimal operating conditions stated in Section 3.4, the conversion of acetic acid using H_2SO_4 and Amberlyst 15 was found to be 98.35% and 87.58%, respectively. In addition, the corresponding conversions were obtained to be 75.26% and 36.12% keeping the fixed reaction time of 1 h. The conversion of acetic acid was 40.85% when the FAC-supported catalyst was used for the fixed reaction time of 1 h. These results revealed that the activity of the FAC-supported catalyst was poor than H_2SO_4 but relatively better than Amberlyst 15. The homogeneous H_2SO_4 catalyst gave more conversion of acetic acid than the FAC-supported catalyst; however, it causes the equipment corrosion, which subsequently will lead to the increase in the cost of the equipment. Thus, it can be

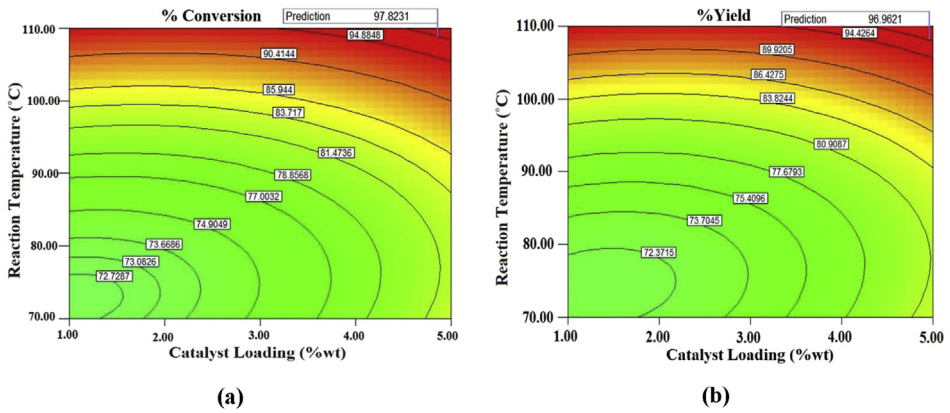

Fig. 6. Contour plots of catalyst loading and reaction temperature with alcohol/acid molar ratio at optimal level for (**a**) % conversion of acid and (**b**) % yield of ester.

inferred that the FAC-supported catalyst has potential to be used for the esterification reaction.

3.6. Catalyst reusability

To study the stability and recyclability of the solid acid catalyst, experiments were performed under optimal reaction conditions. The catalyst was separated from the reaction mixture and washed with *n*-hexane after subsequent reaction cycles. It was then dried in a hot air oven and used to examine its recyclability. The recyclability study revealed that the FAC-supported solid acid catalyst exhibited similar catalytic activity till the third reaction cycle (Fig. 7).

The catalyst started losing its activity after the third reaction cycle. The conversion was observed to be reduced from 89.55% to 58.51% and the yield was reduced from 87.52% to 56.74%. A decline in catalytic activity may be attributed to the deposition of reactants and/or products on the active sites and leaching of active acidic sites from the surface of the solid acid catalyst [3,32].

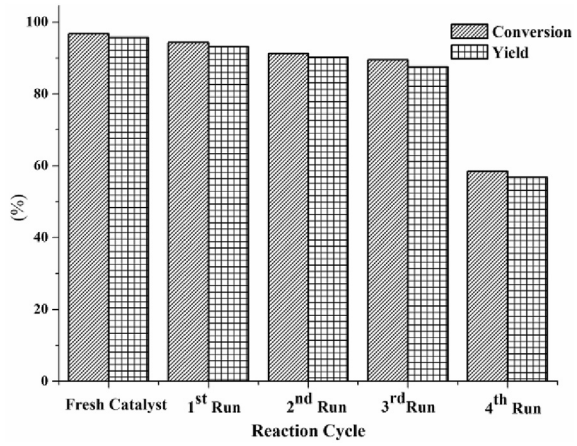

Fig. 7. Reusability of the catalyst in the esterification reaction.

4. Conclusions

The present investigation provides an efficient low-cost solid acid catalyst prepared from cenospheres by the method of wet impregnation by ammonium sulfate. The catalyst exhibited high acidity and catalytic activity for the esterification acetic acid and *n*-octanol. The characterization of the solid acid catalyst confirmed the presence of an adequate amount of silica content and thus surface hydroxyl groups (−OH), which are responsible for surface acidity. It was also observed that the active sites were impregnated on the surface of the catalyst with an enhanced surface area. Response surface methodology was used to optimize the various process parameters for the synthesis of *n*-octyl acetate (flavor ester) catalyzed by the FAC-supported catalyst. The parameters viz., a molar ratio of alcohol/acid and catalyst loading were linearly affected by the esterification reaction, whereas the interaction effect of catalyst loading and the reaction temperature was found to be highly significant. Polynomial model equations were developed to predict the esterification conversion and yield. The prediction of the model was validated experimentally with a good agreement. The FAC-supported catalyst serves as a potential solid acid catalyst for the esterification reaction, which is revealed from the high % conversion of acetic acid (95.34%) and high % yield of *n*-octyl acetate (94.81%). Under optimal operating conditions, the catalyst showed a poor performance than that of H_2SO_4 but a relatively better performance than that of Amberlyst 15. In addition, the catalyst showed a good recyclability with a similar efficacy up to three reaction cycles. This efficient low-cost solid acid catalyst can be used as a replacement of harmful liquid acids for the esterification reactions to synthesize flavor ester. This study explored the use of industrial waste cenospheres for the development of the catalyst for the esterification reactions.

References

[1] R. Kumar, S. Kumar, S.P. Mehrotra, Resour., Conserv. Recycl. 52 (2007) 157–179.

[2] N. Mazumder, R. Rano, G. Sarmah, J. Ind. Eng. Chem. 32 (2015) 211–217.
[3] M.S. Kotwal, P.S. Niphadkar, S.S. Deshpande, V.V. Bokade, P.N. Joshi, Fuel 88 (9) (2009) 1773–1778.
[4] W. Wang, J. Zhai, Q. Li, J. Colloid Interface Sci. 444 (2015) 10–16.
[5] J. Lu, F. Xu, D. Wang, J. Huang, W. Cai, J. Hazard. Mater. 165 (2009) 120–125.
[6] J. Pang, Q. Li, B. Wang, D. Tao, X. Xu, W. Wang, J. Zhai, Powder Technol. 226 (2012) 246–252.
[7] C.V. Ly, D.C. Southam, J. Am. Ceram. Soc. 92 (4) (2009) 881–887.
[8] S. Liu, J. Zhu, X. Guo, J. Ge, H. Wu, Colloids Surf., A 484 (2015) 434–440.
[9] B. Wang, Z. Yang, H. An, J. Zhai, Q. Li, H. Cui, Appl. Surf. Sci. 324 (2015) 817–824.
[10] I. Ju, H. Lim, W. Jeon, D. Suh, M. Park, Y. Suh, Chem. Eng. J. 168 (1) (2011) 293–302.
[11] K.Y. Nandiwale, V.V. Bokade, Ind. Eng. Chem. Res. 53 (49) (2014) 18690–18698.
[12] V.S. Chandane, A.P. Rathod, K.L. Wasewar, S.S. Sonawane, Korean J. Chem. Eng. 34 (1) (2017) 249–258.
[13] V.S. Chandane, A.P. Rathod, K.L. Wasewar, S.S. Sonawane, Korean J. Chem. Eng. 34 (4) (2017) 987–996, http://dx.doi.org/10.1007/s11814-017-0006-4.
[14] Y. Duan, Y. Wu, Y. Shi, M. Yang, Q. Zhang, H. Hu, Catal. Commun. 82 (2016) 32–35.
[15] A. Nagvenkar, S. Naik, J. Fernandes, Catal. Commun. 65 (2015) 20–23.
[16] F. Rajabi, M. Raessi, R.A.D. Arancon, M.R. Saidi, R. Luque, Catal. Commun. 59 (2015) 122–126.
[17] K. Saravanan, B. Tyagi, H.C. Bajaj, Catal. Sci. Technol. 2 (2012) 2512–2520.
[18] D. Rattanaphra, A.P. Harvey, A. Thanapimmetha, P. Srinophakun, Renew. Energy 36 (10) (2011) 2679–2686.
[19] M. Seddighi, F. Shirini, M. Mamaghani, C. R. Chimie 18 (2015) 573–580.
[20] J. Yang, L. Zhou, X. Guo, L. Li, P. Zhang, R. Hong, T. Qiu, Chem. Eng. J. 280 (2015) 147–157.
[21] H.R. Gurav, K.Y. Nandiwale, V.V. Bokade, J. Phys. Org. Chem. 27 (2) (2014) 121–127.
[22] M.A. Olutoye, S.W. Wong, L.H. Chin, H. Amani, M. Asif, B.H. Hameed, Renew. Energy 86 (2016) 392–398.
[23] S.Y. Chen, L. Attanatho, T. Mochizuki, Y. Abe, M. Toba, Y. Yoshimura, C. Kumpidet, P. Somwonhsa, S. Lao-ubol, C. R. Chimie 19 (2016) 1166–1173.
[24] Y. Kuwahara, W. Kaburagi, K. Nemoto, T. Fujitani, Appl. Catal., A 476 (2014) 186–196.
[25] M. Li, D. Chen, X. Zhu, Chin. J. Catal. 34 (9) (2013) 1674–1682.
[26] T.S. Galhardo, N. Simone, M. Goncalves, F.C.A. Figueiredo, D. Mandelli, W.A. Carvalho, ACS Sustainable Chem. Eng. 1 (2013) 1381–1389.
[27] F. Blanco, M.P. Garcia, J. Ayala, Fuel 84 (2005) 89–96.
[28] C. Khatri, A. Rani, Fuel 87 (2008) 2886–2892.
[29] R. Chakraborty, S. Bepari, A. Banerjee, Chem. Eng. J. 165 (3) (2010) 798–805.
[30] W. Mozgawa, M. Król, J. Dyczek, J. Deja, Spectrochim. Acta, Part A 132 (2014) 889–894.
[31] F. Blanco, M.P. Garcia, J. Ayala, G. Mayoral, M.A. Garcia, Fuel 85 (2006) 2018–2026.
[32] B. Tyagi, M.K. Mishra, R.V. Jasra, Catal. Commun. 7 (2006) 52–57.